Arch. Mech., 37, 6, pp. 603–619, Warszawa 1985

Inelastic behaviour of plane frictionless block-systems described as Cosserat media

D. BESDO (HANNOVER)

THE FIRST remarks are concerned with the linearly elastic global behaviour of systems of blocks and springs which should be described as Cosserat media. Basing on these ideas, the inelastic behaviour of frictionless block-systems is treated. They can be models for special rock formations. It is shown that the classical approach leads to results which are in contradiction to experiments. Then the global material behaviour is formulated by means of Cosserat media; conditions for the admissibility of stress fields and for the admissibility of velocity fields and upper and lower bound theorems are developed. Their applications yield results which are in best agreement with experiments.

Na wstępie omówiono globalne własności liniowo sprężyste układów bloczków i sprężynek modelujących ośrodki Cosseratów. Na tej podstawie dyskutuje się niesprężyste właściwości układów bloczków bez tarcia, które mogą symulować zachowanie się pewnych formacji skalnych. Wykazano, że podejście klasyczne prowadzi tu do wyników sprzecznych z doświadczeniem. Sformułowano następnie podstawy globalnego zachowania się materiału za pomocą teorii ośrodków Cosseratów; przedstawiono warunki dopuszczalności pól naprężeń i prędkości oraz twierdzenia o kresach górnych i dolnych. Ich zastosowania prowadzą do wyników zgodnych z doświadczeniami.

В начале обсуждены глобальные линейно упругие свойства систем блочков и пружинок моделирующих среды Коссера. На этой основе обсуждаются неупругие свойства систем блочков без трения, которые могут имитировать поведение некоторых скальных формаций. Показано, что классический подход приводит здесь к результатам противоречащим экспериментам. Затем сформулированы основы глобального поведения материала при помощи теории сред Коссера; представлены условия допустимости полей напряжений и скоростей, а также теоремы о верхних и нижних гранях. Их применения приводят к результатам совпадающим с экспериментами.

1. Introductory remarks on elasticity

IN THE LINEAR theory of plane elastic Cosserat continua, the stresses $\sigma_{\alpha\beta}$ and couple stresses $\mu_{\alpha z}(\alpha = x, y)$ of Fig. 1 occur as well as the strains $\gamma_{\beta\alpha}$, $\varkappa_{z\alpha}$ of Fig. 2. The strains can be derived from displacement fields by

$$
\begin{aligned}
\gamma_{xx} &= \partial u/\partial x,\\
\gamma_{yy} &= \partial v/\partial y,\\
\gamma_{xy} &= \partial u/\partial y+\psi,\\
\gamma_{yx} &= \partial v/\partial x-\psi,\\
\varkappa_{zx} &= \partial \psi/\partial x,\\
\varkappa_{zy} &= \partial \psi/\partial y.
\end{aligned}
\tag{1.1}
$$

The virtual work per unit volume is given by

$$
\delta w = \sigma_{\alpha\beta}\,\delta\gamma_{\beta\alpha}+\mu_{\alpha z}\,\delta\varkappa_{z\alpha}. \tag{1.2}
$$

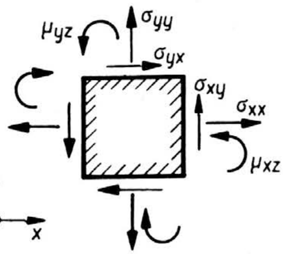

FIG. 1. Definition of stresses.

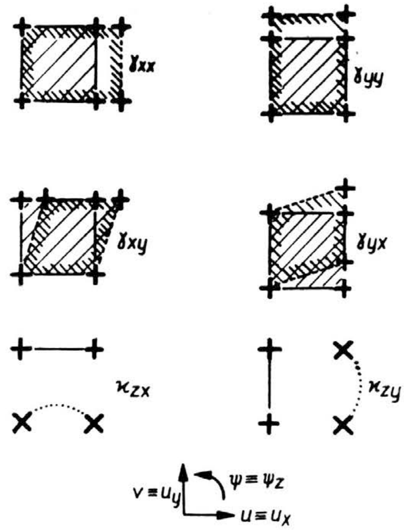

FIG. 2. Definition of strains and displacements.

The linearly elastic theory combines the stresses with the strains by constants. Those constants expressing $\sigma_{\alpha\beta}$ by strains $\gamma_{\beta\alpha}$, are proportional to Young's modulus E, the constants for the combination of $\mu_{\alpha z}$ and $\varkappa_{z\alpha}$ are proportional to E multiplied by the square of a characteristic length L. If this L vanishes the Cosserat-theory turns to a "classical" one.

Hence this length L has to be as large as possible if remarkable differences to the usual theory are to be expected. This can also be expressed by the sentence: The "bending-stiffness" of the medium must be high with respect to the shear-stiffness.

In this paper it will be shown that the concept of a Cosserat-continuum can be an advantageous description of the global behaviour of regularly composed plane structures. Several papers were concerned with grains consisting of circular needles (cf. [1] to [3]). But here the bending stiffness is more or less missing, hence the displacement u and v are almost not influenced by the Cosserat-theory whereas the field of angles ψ is described quite well. As it is well-known, layered media with a high bending-stiffness of the strong bands compared with the shear-stiffness of the weak bands are advantageously described by the concept of Cosserat media.

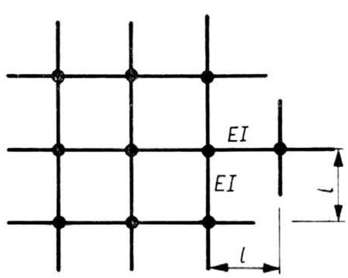

FIG. 3. Usual grid.

On the other hand, frames or grids like that of Fig. 3 seem to be of the typical Cosserat-type, but the "bending-stiffness" of this grid having the thickness b is $EI/(bl)$:

$$\mu_{xz} = \frac{EI}{bl} \varkappa_{zx},$$

whereas the shear-stiffness combining σ_{xy} and γ_{yx} is 12 $EI/(bl^3)$. The typical length L of the Cosserat-continuum is therefore

$$L = \{[EI/(bl)]/[12EI/(bl^3)]\}^{1/2} = l/\sqrt{12}$$

which is a rather small value in comparison with the typical length l of the grid itself. Hence there is no remarkable Cosserat-effect in grids of this type.

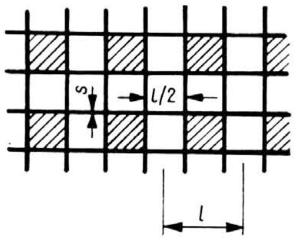

FIG. 4. A special grid.

The situation changes completely if, within this grid, every fourth hole is filled with a rigid material according to the scheme of Fig. 4. Now L depends on l/s which can have high values:

$$\mu_{xz} = \frac{E}{l}\left(\frac{1}{3}s^3 + \frac{1}{4}sl^2\right)\varkappa_{zx}, \qquad \sigma_{xy} = 16\frac{Es^3}{l^3}\gamma_{yx},$$

$$L = l\sqrt{\frac{1}{48} + \left(\frac{l}{8s}\right)^2}.$$

Values of $L = 5l$ can be reached.

More about those special grids and other block-systems and their global elastic behaviour is written in [4] and [5]. The present paper is to point out that the concept of high bending stiffness and relatively low shear stiffness leads to remarkable effects of Cosserat media also in the inelastic case.

2. The inelastic behaviour of frictionless (sliding) blocks

The system of blocks in Fig. 5 can be a model for problems of rock mechanics. It consists of blocks (in experiments wooden and with smooth surfaces) and two lines of gaps or clefts which in nature can be filled with mud. Hence, in the presence of water, an almost frictionless statical state will appear. In the experiments this is approximately realized by pushing on the table or by vibrations.

Under the action of their weight the blocks are pressed together. Hence relative rotations of neighbouring blocks across lines of type 2 are impossible, whereas they are allowed at lines of type 1 in the experiments because of the curved surface of the blocks at their left side. According to these conditions, σ_{xy} and μ_{xz} at lines of type 1 and $\sigma_{\eta\xi}$ at lines of type 2 must vanish, whereas σ_{xx} and $\sigma_{\eta\eta}$ can exist but must be negative. The couple stress

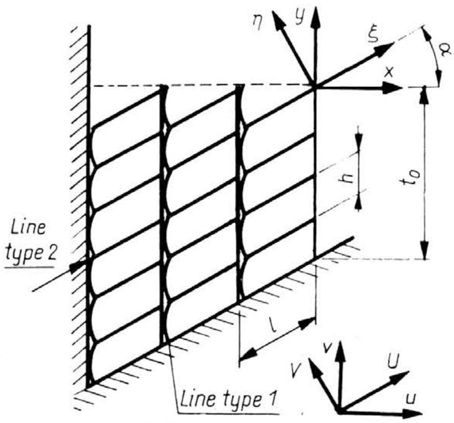

FIG. 5. System of blocks.

$\mu_{\eta\xi}$ can exist but it is bounded because it is derived from the same normal force N as $\sigma_{\eta\eta}$, and N cannot act outside the block:

$$|\mu_{\eta\zeta}| \leq -\frac{l}{2}\sigma_{\eta\eta}. \tag{2.1}$$

If $|\mu_{\eta\zeta}|$ reaches the limit value, the gap will open: the neighbouring blocks can start to rotate against each other.

3. The simple block system

3.1. The "classical" approach

As mentioned above, $\sigma_{xy} = 0$ and $\sigma_{\eta\xi} = 0$ are given; shear stresses vanish in directions other than 90° against each other. Hence, by Mohr's circle it can be seen that shear stresses vanish completely, $\sigma_{xx} = \sigma_{yy}$ has to be fulfilled everywhere.

At the right boundary of the field, $\sigma_{xx} = 0$ has to be satisfied and $\sigma_{yy} = 0$ at the upper surface. The equations of equilibrium reduce by $\sigma_{xy} = \sigma_{yx} = 0$ to

$$\frac{\partial\sigma_{xx}}{\partial x} = 0 \quad \text{and} \quad \frac{\partial\sigma_{yy}}{\partial y} = \gamma$$

(γ = specific weight) and yield

$$\sigma_{xx} \equiv 0 \quad \text{and} \quad \sigma_{yy} = \gamma y.$$

This is in contradiction to $\sigma_{xx} = \sigma_{yy}$. If the system behaved like a "classical" medium, it would break down completely. But the experiments (and intuition) show that the system is stable. Hence the "classical" approach is obviously wrong.

3.2. Relations between stresses in the Cosserat continuum

The virtual work δw of Eq. (1.2) can be expressed by N_1, N_2, M_2, $\delta\Delta u_1$, $\delta\Delta u_2$, $\delta\Delta\psi_2$ (see Fig. 6) acting in the "typical volume" $bhl\cos\alpha$ where b is the thickness of a block:

$$blh\cos\alpha\,\delta w \overset{!}{=} -N_1\,\delta\Delta u_1 - N_2\,\delta\Delta u_2 + M_2\,\delta\Delta\psi_2$$

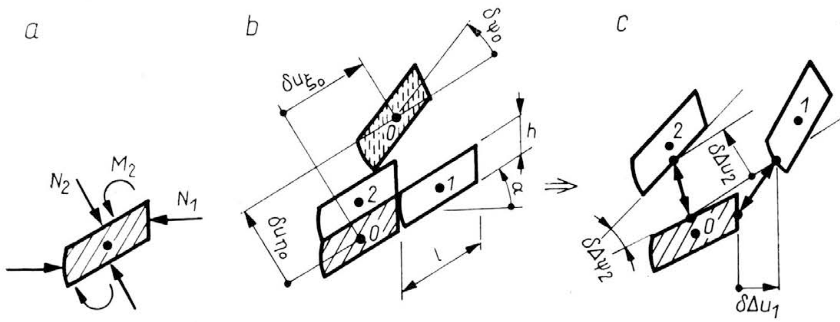

FIG. 6. Basic statical and kinematical properties: a) Forces and torques acting upon a block, b) Position of blocks No 0, 1, 2 in the undeformed state and virtual displacements of block 0, c) Definition of relative virtual displacements.

with

$$\delta\Delta u_1 = (\delta u_{\xi 1} - \delta u_{\xi 0})\cos\alpha - \left[\left(\delta u_{\eta 1} - \frac{l}{2}\,\delta\psi_1\right) - \left(\delta u_{\eta 0} + \frac{l}{2}\,\delta\psi_0\right)\right]\sin\alpha$$

etc. Hence the variations $\delta\Delta u_1$, $\delta\Delta u_2$ and $\delta\Delta\psi_2$ can be approximated by

$$\begin{aligned}\delta\Delta u_1 &= l(\delta\gamma_{\xi\xi}\cos\alpha - \delta\gamma_{\eta\xi}\sin\alpha),\\ \delta\Delta u_2 &= h(\delta\gamma_{\eta\eta}\cos\alpha + \delta\gamma_{\eta\xi}\sin\alpha),\\ \delta\Delta\psi_2 &= h(\delta\varkappa_{\zeta\eta}\cos\alpha + \delta\varkappa_{\zeta\xi}\sin\alpha).\end{aligned} \tag{3.1}$$

The relations (3.1) and (1.2) inserted in Eq. (2.1) yield because of the independence of $\delta\gamma_{\alpha\beta}$, $\delta\varkappa_{\zeta\alpha}$;

$$\begin{gathered}\sigma_{\xi\xi} = -\frac{N_1}{bh}, \quad \sigma_{\eta\eta} = -\frac{N_2}{bl}, \quad \sigma_{\xi\eta} = \left(\frac{N_1}{bh} - \frac{N_2}{bl}\right)\tan\alpha, \quad \sigma_{\eta\xi} = 0,\\ \mu_{\xi\xi} = \frac{M_2}{bl}\tan\alpha, \quad \mu_{\eta\zeta} = \frac{M_2}{bl}.\end{gathered} \tag{3.2}$$

The application of the transformation laws yields

$$\begin{gathered}\sigma_{xx} = -\frac{N_1}{bh}, \quad \sigma_{yy} = -\frac{N_2}{bl}, \quad \sigma_{xy} = 0, \quad \sigma_{yx} = \left(\frac{N_2}{bl} - \frac{N_1}{bh}\right)\tan\alpha,\\ \mu_{xz} = 0, \quad \mu_{yz} = \frac{M_2}{bl}/\cos\alpha.\end{gathered} \tag{3.3}$$

As was assumed above, $\sigma_{\eta\xi} = \sigma_{xz} = \mu_{xz} = 0$ comes out by this theory, too. The normal forces N_1, N_2 can never be negative and $|M_2|$ cannot exceed $-1/2\; N_2 l$. Hence we can derive from Eqs. (3.2) and (3.3) with these conditions:

$$\begin{gathered}\sigma_{\xi\eta} = (\sigma_{\eta\eta} - \sigma_{\xi\xi}\tan\alpha), \quad \sigma_{yx} = (\sigma_{xx} - \sigma_{yy})\tan\alpha = -\sigma_{\xi\eta},\\ \sigma_{\xi\xi} = \sigma_{xx}, \quad \sigma_{\eta\eta} = \sigma_{yy}, \quad \sigma_{\eta\xi} = \sigma_{xy} = \mu_{xz} = 0\end{gathered} \tag{3.4}$$

and

$$\sigma_{\xi\xi} \leq 0, \quad |\mu_{\eta\zeta}| + \frac{l}{2}\sigma_{\eta\eta} = |\mu_{yz}|\cos\alpha + \frac{l}{2}\sigma_{yy} \leq 0. \tag{3.5}$$

These relations have to be satisfied in every admissible stress field.

3.3. An admissible stress field

The boundary conditions for an admissible stress field are (cf. Fig. 7):

I) $\sigma_{xy} = \mu_{xz} = 0$ (valid by the relations (3.3));

II) $\sigma_{yx} = \sigma_{yy} = \mu_{yz} = 0$: here no stresses appear at all;

III) $\sigma_{xy} = \mu_{xz} = \sigma_{xx} = 0$;

IV) no restriction.

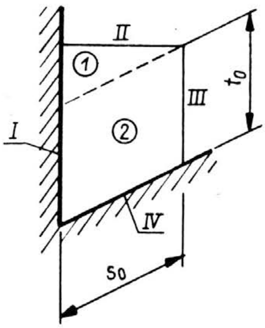

FIG. 7. Zones and boundaries of the field.

With $\sigma_{xz} = \sigma_{\eta\xi} = 0$ the equations of equilibrium reduce to

$$\frac{\partial \sigma_{xx}}{\partial x} + \frac{\partial \sigma_{yx}}{\partial y} = 0, \tag{3.6}$$

$$\frac{\partial \sigma_{yy}}{\partial y} = \gamma \tag{3.7}$$

or

$$\frac{\partial \sigma_{\xi\xi}}{\partial \xi} = \gamma \sin\alpha, \tag{3.8}$$

$$\frac{\partial \sigma_{\xi\eta}}{\partial \xi} + \frac{\partial \sigma_{\eta\eta}}{\partial \eta} = \gamma \cos\alpha, \tag{3.9}$$

and

$$\frac{\partial \mu_{\xi\zeta}}{\partial \xi} + \frac{\partial \mu_{\eta\zeta}}{\partial \eta} + \sigma_{\xi\eta} = 0 \tag{3.10}$$

or

$$\frac{\partial \mu_{yz}}{\partial y} - \sigma_{yx} = 0. \tag{3.11}$$

In connection with the boundary conditions, Eqs. (3.7) and (3.8) yield

$$\sigma_{yy} = \gamma y \tag{3.12}$$

and

$$\sigma_{\xi\xi} = \sigma_{xx} = q \sin\alpha(\xi - \xi_0(\eta)) = \begin{cases} \gamma y & \text{in } \mathit{1}, \\ \gamma x \tan\alpha & \text{in } \mathit{2}, \end{cases} \tag{3.13}$$

hence also

$$\sigma_{yx} = (\sigma_{xx} - \sigma_{yy})\tan\alpha = \begin{cases} 0 & \text{in } 1, \\ \gamma(x\tan\alpha - y)\tan\alpha & \text{in } 2, \end{cases}$$

and

$$\mu_{yz} = \begin{cases} 0\,. & \text{in } 1, \\ -\frac{1}{2}\gamma\tan\alpha(y - x\tan\alpha)^2 & \text{in } 2. \end{cases}$$

With $y = -|y| \le 0$, the second condition (3.5) yields

$$\sin\alpha(y - x\tan\alpha)^2 \leqq l|y|.$$

With increasing t_0 (see Fig. 7), the first failure will occur at $y = -t_0$, $x = 0$; hence,

(3.14) $$t_0 \le l/\sin\alpha$$

denotes an upper bound for the depth of admissible stress fields of this type. In experiments $l = 2h$ and $\tan\alpha = 1/2$ were given and these values lead to

(3.15) $$t_0 \le 2\sqrt{5}h = 4{,}472h.$$

The experiments show that the system with 4 blocks at the right side is stable; at 5 or at least at 6 blocks the right column of blocks begins to rotate combined with sliding. This is in complete agreement with the relation (3.15).

3.4. Kinematical conditions and an admissible velocity field

Equations (3.3) and (3.4) and the condition (3.5) can be rewritten as

(3.16) $$|\mu_{xz}| \le 0 \quad (\text{replacing } \mu_{xz} \equiv 0),$$

(3.17) $$|\sigma_{xy}| \le 0,$$

(3.18) $$|(\sigma_{yy} - \sigma_{xx})\sin\alpha\cos\alpha + \sigma_{yx}\cos^2\alpha - \sigma_{yx}\sin^2\alpha)| \leqq 0,$$

(3.19) $$\sigma_{xx} \le 0,$$

(3.20) $$\frac{2}{l}|\mu_{yz}|\cos\alpha + \sigma_{yy}\cos^2\alpha + \sigma_{xx}\sin^2\alpha - (\sigma_{xy} + \sigma_{yx})\sin\alpha\cos\alpha \leqq 0.$$

In this form they have the structure of usual yield conditions in plasticity. The normallity rule yields:

from the relation (3.16): $\dot{\varkappa}_{zy}$ is arbitrary, what is obviously correct for the experiment;

from the relation (3.17) $\dot{\gamma}_{yx} = \partial v_y/\partial x - \omega$ is arbitrary (also obviously);

from the relation (3.18): in addition to other strain rates $\dot{\gamma}_{xy} = \varphi\sin\alpha\cos\alpha$, $\dot{\gamma}_{xx} = -\varphi\sin\alpha\cos\alpha$, $\dot{\gamma}_{xy} = \varphi\cos^2\alpha$, $\dot{\gamma}_{yx} = -\varphi\sin^2\alpha$ with arbitrary φ is possible. After transformation to ξ, η-coordinates, this allows identically for an additional $\dot{\gamma}_{\xi\eta} = \gtreqless 0$, which is obvious, too;

from the relation (3.19): if $\sigma_{xx} = 0$ is valid, an additional $\dot{\gamma}_{xx} \ge 0$ can appear;

from the relation (3.20): if $|\mu_{yz}|\cos\alpha + \frac{1}{2}l\sigma_{\eta\eta} = 0$ is valid, additional $\frac{\partial\omega}{\partial y} = \pm\chi\frac{2}{l}\cos\alpha$ and $\frac{\partial v_\eta}{\partial\eta} = \chi \ge 0$ may occur. This is exactly the kinematical condition for the opening of the gap between to neighbouring blocks in the y-direction.

As the final result it can be stated that every velocity field is admissible which satisfies the following two conditions:

$$\dot{\gamma}_{yy}-\dot{\gamma}_{xy}\tan\alpha-\frac{l}{2}\left|\frac{\dot{\varkappa}_{zy}}{\cos\alpha}\right| = \dot{\gamma}_{\eta\eta}+\dot{\gamma}_{\eta\xi}\tan\alpha-\frac{l}{2}\left|\dot{\varkappa}_{\zeta\eta}-\dot{\varkappa}_{\zeta\xi}\tan\alpha\right| \geq 0 \tag{3.21}$$

and

$$\dot{\gamma}_{xx}+\dot{\gamma}_{xy}\tan\alpha = \dot{\gamma}_{\xi\xi}-\dot{\gamma}_{\eta\xi}\tan\alpha \geq 0.$$

Using the velocity components u, v in the x, y-directions or U, V in the ξ, η-directions, the conditions (3.21) read:

$$\frac{\partial v}{\partial y}-\left(\frac{\partial u}{\partial y}+\omega\right)\tan\alpha-\frac{l}{2\cos\alpha}\left|\frac{\partial\omega}{\partial y}\right| \geq 0$$

or

$$\frac{\partial V}{\partial\eta}+\left(\frac{\partial V}{\partial\xi}-\omega\right)\tan\alpha-\frac{l}{2}\left|\frac{\partial\omega}{\partial\eta}-\frac{\partial\omega}{\partial\xi}\tan\alpha\right| \geq 0 \tag{3.22}$$

and

$$\frac{\partial u}{\partial x}+\left(\frac{\partial u}{\partial y}+\omega\right)\tan\alpha \geq 0 \quad \text{or} \quad \frac{\partial U}{\partial\xi}-\left(\frac{\partial V}{\partial\xi}-\omega\right)\tan\alpha \geq 0.$$

One admissible field with velocity jumps at the boundaries I and II of Fig. 8 and valid in the shadowed area is

$$\begin{aligned} \omega &= -\Omega = \text{const} < 0, \\ u \equiv u(x) &= \Omega(x+\Delta x)\tan\alpha, \\ v &= \Omega\,\frac{l}{2\cos\alpha}+(x+\Delta x)\tan^2\alpha-\tan\alpha(y+\Delta y-x\tan\alpha). \end{aligned} \tag{3.23}$$

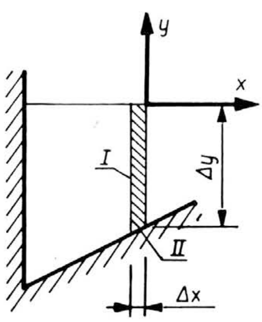

FIG. 8. Area of definition of the velocity field.

4. Upper and lower bound theorems

If the normality rule can be applied, also the different forms of upper and lower bound theorems should have sense. These make use of the fact that the external power of any external force F^* belonging to an internal stress field σ^*, with an arbitrary velocity field v^{**}, is equal to the inner power of the stresses σ^* combined with the strain rates $\dot{\gamma}^{**}$ which are compatible with the velocity field v^{**}

$$P_{\mathrm{ex}}(F^*, v^{**}) = P_{\mathrm{in}}(\sigma^*, \dot{\gamma}^{**}).$$

From the normality rule and from the uniqueness of the material behaviour, the inequalities ($\hat{}$ denoting "true" values)

$$P_{in}(\sigma, \hat{\dot{\gamma}}) \leq P_{in}(\hat{\sigma}, \hat{\dot{\gamma}}) \quad \text{and} \quad P_{in}(\sigma(\gamma), \gamma) \geq P_{in}\hat{\sigma}(, \hat{\dot{\gamma}})$$

can be derived. Furthermore, in the case of the sliding blocks, it is obvious that $P_{in}(\sigma(\dot{\gamma}), \dot{\gamma})$ and $P_{in}(\hat{\sigma}, \hat{\dot{\gamma}})$ vanish; hence the remaining relations are in the best applicable form:

(4.1) *lower bound theorem*: $P_{ex}(F, \hat{v}) = P_{in}(\sigma, \hat{\dot{\gamma}}) \leq 0$,

(4.2) *upper bound theorem*: $P_{ex}(\hat{F}, v) \leqq 0$.

These relations need an interpretation:

RELATION (4.1)

F can stand for a set of given external forces to an arbitrary admissible stress field, $\hat{v}$ stands for one of the numerous admissible velocity fields describing all possible real motions. If the combination yields $P_{ex}(F, \hat{v}) < 0$ for each of those fields $\hat{v}$, the forces F cannot induce motion at all. If $P_{ex}(F, \hat{v}) = 0$ can be reached in a appropriate combination, also $P_{in}(\sigma, \hat{\dot{\gamma}})$ and hence the local $P_{in}(\sigma, \hat{\dot{\gamma}})$ vanishes. Therefore, then F, σ, $\hat{v}$, and $\hat{\dot{\gamma}}$ form "the" quasi-static solution. Hence:

SENTENCE A

If a (statically) admissible stress field exists for given (!) external forces, it belongs to a quasi-statical solution or cannot induce motion at all. Accelerations are then impossible.

RELATION (4.2)

SENTENCE B

If an admissible velocity-field v induces $P_{ex}(\hat{F}, v) > 0$ with given external forces $\hat{F}$, there does not exist any quasi-static solution with these external forces. Accelarations will then occur.

The application of these sentences with respect to the stress field of Sect. 3.3 and the velocity field (3.23) produces:

SENTENCE A. As long as t_0 is not higher than $l/\sin\alpha$, the system is not unstable.

SENTENCE B. The external forces $\hat{F}$ are the specific weight γ in the y-direction. Hence $P_{ex}(\hat{F}, v)$ is in this case

$$P_{ex}(\hat{F}, v) = b \iint\limits^{A} -\gamma v \, dx\, dy.$$

The result of the integration over the shadowed area of Fig. 8 is

$$P_{ex}(\hat{F}, v) = -\Omega b\gamma \frac{\Delta x}{2\cos\alpha}\left[\Delta y(l - \Delta y \sin\alpha) + \frac{1}{2}\Delta x l \tan\alpha\right].$$

If Δx tends to zero,

$$\Delta y = t_0 \leq l/\sin\alpha$$

is necessary.

As a conclusion: $t_0^* = l/\sin\alpha$ is at the same time the upper and the lower bound of the possible depth t_0. This is in best agreement with experiments (cf. the photos of Fig. 9).

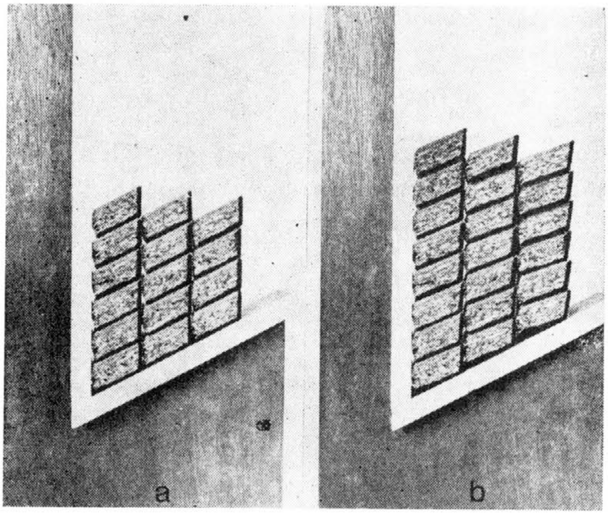

FIG. 9. Experiment with the simple block system a) $t_0 < 4.5h$: stable, b) $t_0 > 4.5h$: rotation.

5. A less trivial problem

5.1. The problem and the classical approach

In the second example of this paper, the field is filled with blocks of the same type as in Sect. 3. But with the help of several half-blocks the new structure of Fig. 10a is put together. In this case only $\sigma_{\eta\xi} = 0$ is obvious in the absence of friction. Within the classical approach this implies $\sigma_{\xi\eta} = 0$. Hence then only $\sigma_{\xi\xi}$ and $\sigma_{\eta\eta}$ exist, but they may be different.

The statical boundary-conditions at I, II, III of Fig. 10b are

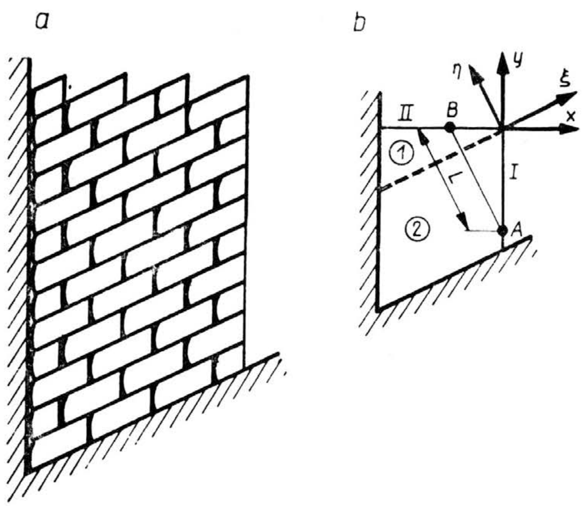

FIG. 10. A less trivial problem: a) structure, b) geometrical definitions.

I) $\sigma_{xx} = \sigma_{xy} = 0 \quad \rightarrow \quad \sigma_{\xi\xi} = \sigma_{\eta\eta} = 0,$

II) $\sigma_{yx} = \sigma_{yy} = 0 \quad \rightarrow \quad \sigma_{\xi\xi} = \sigma_{\eta\eta} = 0,$

III) $\sigma_{xy} = 0 \quad \rightarrow \quad \sigma_{\xi\xi} = \sigma_{\eta\eta}.$

The equations of equilibrium yield

$$\partial\sigma_{\xi\xi}/\partial\xi = \gamma\sin\alpha \rightarrow \sigma_{\xi\xi} = \ldots \leq 0 \text{ (this is o.k.)}$$

and

$$\partial\sigma_{\eta\eta}/\partial\eta = \gamma\cos\alpha \rightarrow \sigma_{\eta\eta}(B) = \sigma_{\eta\eta}(A) + L\gamma\cos\alpha \qquad \text{(Fig. 10b).}$$

The second result is in contradiction to the boundary condition at A and B. Hence there cannot exist any stable "classical" solution if lines as A – B belong to the field.

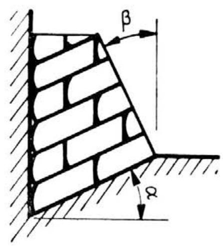

FIG. 11. Bound for classical solutions.

Systems like that of Fig. 11 with $\beta \geqslant \alpha$ can have a "stable" classical solution. But experiments show that the system of Fig. 10 is also stable.

Hence the steps of Sect. 3 will now be repeated for the second system.

5.2. Conditions for the stresses

Each block of the field has in this case three pairs of neighbouring blocks, and N_1, N_2, N_3 as well as M_2, M_3 exist. These forces and moments are bounded by the conditions

$$N_1 \geq 0, \quad N_2 \geq \frac{4}{l}|M_2|, \quad N_3 \geq \frac{4}{l}|M_3|. \tag{5.1}$$

The application of the virtual work theorem now yields:

$$\begin{gathered} N_1 = -\sigma_{\xi\xi}bh, \quad N_2 = -\frac{1}{2}\sigma_{\eta\eta}bl - \frac{\sigma_{xy}}{\cos\alpha}bh, \quad N_3 = -\frac{1}{2}\sigma_{\eta\eta}bl + \frac{\sigma_{xy}}{\cos\alpha}bh, \\ M_2 = \frac{1}{2}\mu_{\eta\zeta}bl + \mu_{xz}bh, \quad M_3 = \frac{1}{2}\mu_{\eta\zeta}bl - \mu_{xz}bh. \end{gathered} \tag{5.2}$$

The other stresses in ξ, η-coordinates can always be computed by

$$\sigma_{\eta\xi} = 0, \quad \sigma_{\xi\eta} = \frac{\sigma_{xy}}{\cos^2\alpha} + (\sigma_{\eta\eta} - \sigma_{\xi\xi})\tan\alpha, \quad \mu_{\xi\zeta} = \frac{\mu_{xz}}{\cos\alpha} + \mu_{\eta\zeta}\tan\alpha. \tag{5.3}$$

For the further description, s and t are introduced according to Fig. 13, and the following abbreviations are defined:

$$\frac{\sigma_{xy}}{\cos\alpha} = -P\gamma, \quad \sigma_{\eta\eta} = -Q\gamma, \quad \mu_{xz} = p\gamma, \quad \mu_{\eta\zeta} = q\gamma. \tag{5.4}$$

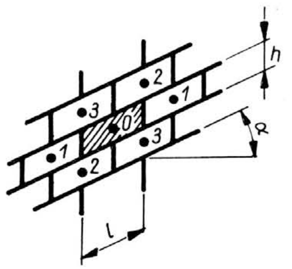

FIG. 12. Numbers of blocks.

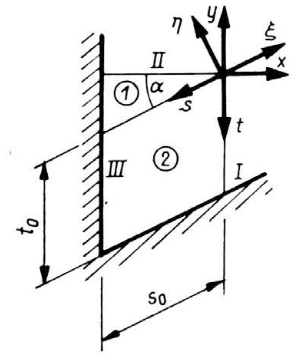

FIG. 13. Introduction of s, t-coordinates.

The equations of equilibrium yield first

(5.5) $$\sigma_{\xi\xi} = -\big(s-s_1(t)\big)\gamma\sin\alpha \leqq 0$$

with

(5.6) $$s_1(t) = \begin{cases} t/\sin\alpha & \text{in } 1\,, \\ 0 & \text{in } 2\,. \end{cases}$$

The other equations of equilibrium can then be written as

(5.7) $$\begin{aligned} &\frac{\partial P}{\partial s} + \frac{\partial Q}{\partial t} = 1, \\ &\frac{\partial p}{\partial s} + \frac{\partial q}{\partial t} = -P - Q\sin\alpha + \big(s-s_1(t)\big)\sin^2\alpha, \end{aligned}$$

whereas the remaining conditions (5.1) are

(5.8) $$|q+Hp| \leq \frac{l}{4}(Q+HP) \quad \text{and} \quad |q-Hp| \leq \frac{l}{4}(Q-HP)$$

with

(5.9) $$H = 2h/l.$$

On the boundaries I, II, and III (cf. Fig. 13) the following conditions have to be satisfied:

(5.10) $$\begin{aligned} &\text{I)} \quad p = P = \sigma_{\xi\xi} = 0, \\ &\text{II)} \quad q + p\sin\alpha = Q + P\sin\alpha = \sigma_{\xi\xi} = 0, \\ &\text{III)} \quad p = P = 0. \end{aligned}$$

5.3. Admissible stress fields

A first stress field satisfying Eqs. (5.7) and (5.10) is that of Sect. 3. It has to be rewritten as

(5.11) $$P = p = 0, \quad Q = t + s\sin\alpha, \quad q = \begin{cases} 0 & \text{in } 1\,, \\ -\dfrac{1}{2}t^2\sin\alpha & \text{in } 2\,. \end{cases}$$

The conditions (5.8) reduce to one: $\frac{1}{2}t^2\sin\alpha \leqslant \frac{l}{4}(t+s\sin\alpha)$, hence:

$$t \leq l/(2\sin\alpha). \tag{5.12}$$

This limit for t has only half the value of the relation (3.14) for the other example. But experiments show that higher limits of t should be possible. In this sense the limit of the relation (5.12) is a correct lower bound for admissible values of t_0, but it is not satisfactory.

In the opposite to Sect. 3, here possibilities for an optimization of the limiting value exist because 4 fields of stress-variables (P, Q, p, q) are to be chosen and are governed by two equations (5.7) and two conditions (5.8) only. No numerical optimization procedures have been applied until now, but a better stress field has been found intuitively basing on experimental facts.

The computed field is admissible for $s_0 = 3.5\ l$, $t_0 = s_0/(2\sin\alpha)$, $H = 1$, and $\tan\alpha = 1/2$. These values are chosen in connection with the experiments. The field consists

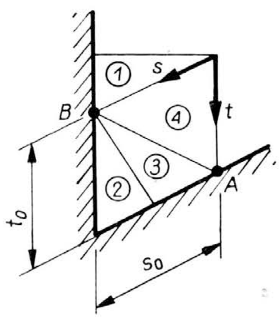

FIG. 14. Regions of the stress-field.

of four parts (cf. Fig. 14): In three of them p and q vanish, only in 4 these quantities differ from zero

$$\begin{aligned}
1:&\quad P = 0,\quad Q = t+s\sin\alpha,\\
2:&\quad P = s-s_0,\quad Q = (s_0-s\cos^2\alpha)/\sin\alpha,\\
3:&\quad P = s_0-s-2t\sin\alpha,\\
&\quad Q = 2t-s_0/\sin\alpha+s(1/\sin\alpha+\sin\alpha),\\
4:&\quad s_g(t) := s_0(1-t/t_0),\\
&\quad P = -\frac{1}{2}\left\{\left(s_0/s_g(t)\right)^2-1\right\}s,\\
&\quad Q = (4\sin\alpha)^{-1}\{s_0/s_g(t)-s_g(t)\}+s\sin\alpha,\\
&\quad p = \frac{s_0^2}{8}(1-\varrho)\{[-2(1+\varrho)+\varrho(1+3\varrho)T](\nu-\nu^2)-T(1-\varrho^2)\nu^2\},\\
&\quad q = \frac{\sqrt{5}}{16}Ts_0^2(1-\varrho)(1-\varrho^2)(1-2\nu),
\end{aligned}$$

where $\varrho = 1-t/t_0$ and $\nu = s/s_g(t)$. T is chosen as $T = 0.86$. As it can easily be verified, Eqs. (5.7) and the conditions of transition are satisfied; moreover, the condition (5.8) in *1*, *2* and *3* can be proved trivially, but in region *4* the proof of the conditions (5.8) is troublesome, nevertheless, it is possible.

The most surprising fact of this stress field is that it contains a single force acting at A (cf. Fig. 14). Further on, jumps of stresses along line $A-B$ appear. The fields of P, Q and the quotients

$$W_{1,2} = (q \pm Hp)/(Q \pm HP)$$

are plotted in Fig. 15.

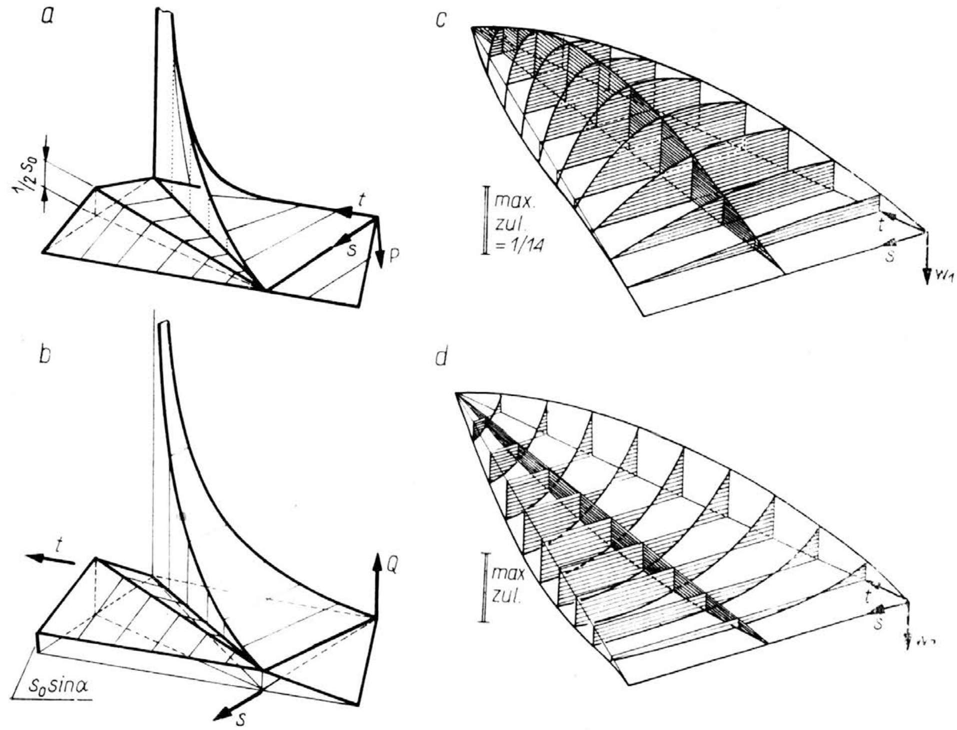

FIG. 15. An admissible stress-field, plots: a) P, b) Q, c) w_1 d) w_2.

From this field a new limiting value for t_0 can be derived:

$$t_0 \leq \frac{s_0}{2\sin\alpha} = \frac{\sqrt{5}}{2} s_0 = \frac{7}{4}\sqrt{5}l = \frac{7}{2}\sqrt{5}h = 7.826h.$$

This is, however, also only a lower bound for this limiting value which, according to the experiments, should be nearer to $10h$.

5.4. Kinematical conditions and bounds

The kinematical conditions corresponding to the conditions (3.21) are now

$$\dot{\gamma}_{\xi\xi} - \dot{\gamma}_{\eta\xi} \tan\alpha \geq 0$$

and

$$H(\dot{\gamma}_{\eta\eta}+\dot{\gamma}_{\eta\xi}\tan\alpha)\pm\dot{\gamma}_{\eta\xi} \geq \frac{l}{4}\,|H(\dot{\varkappa}_{\zeta\eta}+\dot{\varkappa}_{\zeta\xi}\tan\alpha)\pm\dot{\varkappa}_{\zeta\xi}|.$$

These conditions are satisfied by the following velocity field defined in the shadowed areas of Fig. 16 and containing admissible jumps of the velocities along the boundaries I and II.

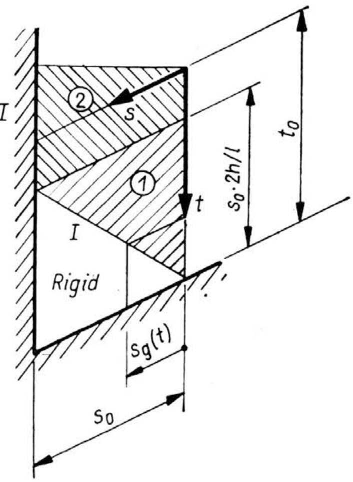

FIG. 16. Zones of the second velocity field.

The angular velocity is assumed to be negative and constant:

$$\omega = -\Omega = \text{const},$$

the velocities U and V are

$$U = \Omega\tan\alpha\left\{\frac{l}{4}-(t_0-t)\sin\alpha+s_g(t)\right\},$$

$$V = \Omega\left\{\frac{l}{4}-(t_0-t)\sin\alpha+s\right\},$$

where $s_g(t)$ is

$$s_g(t) = \begin{cases} \dfrac{l}{2h}(t_0-t) & \text{in } 1, \\ s_0 & \text{in } 2. \end{cases}$$

For the computation of $P_{ex}(\hat{F}, v)$, the component v is needed:

$$v = \frac{\Omega}{\cos\alpha}\left\{\frac{l}{4}-(t_0-t)\sin\alpha+s\cos^2\alpha+s_g(t)\sin^2\alpha\right\}.$$

The integration of $P_{ex}(\hat{F}, v)$ has the result

$$P_{ex}(\hat{F}, v) = -\frac{b\Omega}{\cos\alpha}\left\{\frac{l}{4}\left[s_0t_0-\frac{1}{2}s_0^2(1-\sin\alpha)\right]-\frac{1}{2}s_0t_0^2\sin\alpha + \frac{1}{2}s_0^2t_0+s_0^3\left[\frac{1}{2}\sin\alpha-\frac{1}{3}(1+\sin^2\alpha)\right]\right\} \leq 0.$$

It has — as it is necessary — a negative value for $s_0 = t_0$ and $2h/l = 1$. The limiting value $P_{ex}(\hat{F}, v) = 0$ is reached for

$$\frac{t_0}{s_0} = \frac{1}{\sin\alpha}\left\{\left(\frac{1}{2}+\frac{l}{4s_0}\right) \pm \sqrt{\left(\frac{1}{2}+\frac{l}{4s_0}\right)^2 + \sin^2\alpha - \frac{2}{3}\sin\alpha - \frac{2}{3}\sin^3\alpha + \frac{l}{4s_0}\sin\alpha(1-\sin\alpha)}\right\}.$$

For $l/(4s_0) = 1/14$ and $\tan\alpha = 1/2$, this upper limit for t_0 is:

$$t_0 \leq 2.1470 s_0 = 15.03h.$$

As the final result for the problem of this chapter, it can be stated that systems are stable if and only if $t_0 \leqq t_{lim}$ is valid and that this limiting value has to be in the range of

$$7.826h \leq t_{lim} \leqslant 15.03h.$$

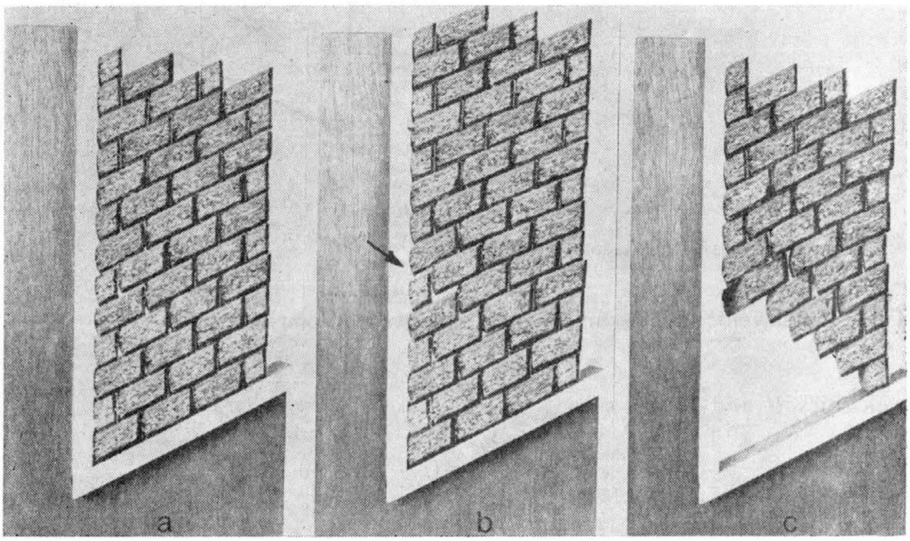

FIG. 17. Experiments with the less trivial system: a) $t_0 = 10h$: undeformed (with friction), b) $t_0 = 10h$: after "deformation" (overstressed by additional loads), c) single force at the right corner: A lot of blocks can be put out.

The experiments (see the photos of Fig. 17) show that the real value of t_{lim} lies near 10 h. That the range in which t_{lim} can vary theoretically is not smaller, follows from the fact that no optimization procedures have been applied up to now. The solutions will have to be improved in this direction in the future.

If the fact that half-blocks appear is better taken into account also in the upper bound calculations, the final result is

$$7.826h \leq t_{lim} \leq 13.18h.$$

6. Conclusions

It has been shown that the global behaviour of special systems of frictionless blocks cannot be described properly by a classical approach. But these systems being models for possible formations of rocks with clefts are described very well by means of Cosserat continua.

The application of upper and lower bound theorems derived here, leads in one simple example to a definite value of a limit for the height of a step in the landscape which is in best agreement with the result of appropriate experiments. In a less trivial problem, this limit can only be bounded in a relatively wide range. Here numerical optimization procedures have to be applied in the future in order to reach better bounds.

References

1. D. BESDO, *Slip-line methods of numerical analysis in plane deformations of rigid/plastic, isotropic, incompressible Cosserat continua*, Mech. Rs. Com., 1, 155–160, 1974.
2. N. BOGDANOVA-BONTCHEVA and H. LIPPMANN, *Rotationally symmetric plane flow of granular materials*, Acta Mech., 1975.
3. M. BECKER and W. HAUGER, *Granular material—an experimental realization of a plastic Cosserat-continuum*, in: Mechanics of Inelastic Media and Structure, O. MAHRENHOLTZ and A. SAWCZUK [ed.], PWN, Warszawa-Poznań 1982.
4. D. BESDO, Zur Beschreibung von ebenen Blockstrukturen als Cosserat-Kontinua, Z. Angew. Mech., Math. 65, 4, 1985.
5. U. von Broock, *Zur Angewendung des elastischen Cosserat-Kontinuums bei regelmässing strukturierten Scheiben*, Fortschr. Ber. Z-VDI, Reihe 1, Nr 92.

INSTITUT FÜR MECHANIK,
UNIVERSITÄT HANNOVER, FRG.

Received March 18, 1985.